

Ultra wide black-hole - neutron star binaries as a possible source for gravitational waves and short gamma ray bursts

EREZ MICHAELY^{1,2} AND SMADAR NAOZ^{1,2}

¹*Department of Physics and Astronomy, University of California, Log Angeles, CA 90095, USA*

²*Mani L. Bhaumik Institute for Theoretical Physics, University of California, Log Angeles, CA 90095, USA*

ABSTRACT

The third observing run of the LIGO/Virgo/KARGA collaboration reported a few neutron star–black hole (NSBH) merger events. While NSBH mergers have yet to receive extensive theoretical attention, they may have a promising electromagnetic signature in the form of short gamma-ray bursts. Here we show that NSBH dynamical mergers can naturally form from ultra-wide binaries in the field. Flyby gravitational interactions with other neighbors in the galaxy in these ultra-wide systems may result in high eccentricity that drives the binary into a merger. We show that this process can result in a merger rate at the order of $\sim 10 \text{ Gpc}^{-3} \text{ yr}^{-1}$ ($\sim 5 \text{ Gpc}^{-3} \text{ yr}^{-1}$) for elliptical (spiral) galaxies. This channel predicts higher merger rate with higher velocity dispersion of the host-galaxy, delay time distribution which shallower than uniform but steeper than $1/t$, higher merger rate for lower BH to NS mass ratio.

Keywords: gravitational waves () — stars: kinematics and dynamics — stars: neutron — stars: black holes

1. INTRODUCTION

With the recent third catalog of observed gravitational waves signals was published (The LIGO Scientific Collaboration et al. 2021a), a total of 90 GW candidates were detected, which allows a significant improvement of the inferred merger rates for each of the three classes of binary systems, Binary Black-hole (BBH), Binary neutron stars (BNS) and black-hole (BH) neutron star (NS) binary (BHNS). The LIGO-VIRGO-KARGA collaboration (The LIGO Scientific Collaboration et al. 2021b) report that the for the BBH class the merger rate is $17.3 - 45 \text{ Gpc}^{-3} \text{ yr}^{-1}$, for the BNS the inferred rate is $13 - 1900 \text{ Gpc}^{-3} \text{ yr}^{-1}$ and for the BHNS the corresponding rate is $7.4 - 320 \text{ Gpc}^{-3} \text{ yr}^{-1}$.

The formation of GW sources can roughly be divided into four groups:

(1) Isolated stellar binary: In this channel, massive stellar binaries evolve together, in the absence of additional dynamical interaction (e.g., Dominik et al. 2015; de Mink & Belczynski 2015; Belczynski et al. 2016; Eldridge et al. 2017; Giacobbo et al. 2018; Olejak et al.

2020), or via stable mass transfer (e.g. Gallegos-Garcia et al. 2021). Fraction of the close massive binaries evolve through one or two common envelope process resulting in a possible formation of short period binary. Some fraction of these system are sufficiently close to merge by the emission of GW within Hubble time. A well known challenge to this avenue is the common envelope phase which may cause the binary to merge before the formation of the compact objects. However, a proposed avenue that may overcome this challenge may lay in the form of chemically homogeneous stellar evolution which may avoid mass transfer (e.g., Marchant et al. 2016; de Mink & Mandel 2016; Mandel & de Mink 2016).

(2) Dynamical mergers in dense environments. Dense environments are efficient in producing many binary exotica due to the high stellar density. Galactic centers, or globular clusters and even low mass young clusters and open clusters are heavily populated with stellar and compact objects. In these environments, stars and compact objects, both singles and binaries experience strong gravitational interactions with individual stars or with higher multiplicity systems. These interactions tend to harden hard binaries, and possibly unbind soft binaries (Heggie 1975), whilst change their eccentricities. As a results some fraction of these binaries may merge via GW emission in a Hubble time (e.g.,

Antonini & Perets 2012; Samsing et al. 2014; Rodriguez et al. 2016, 2018, 2021; Fragione & Kocsis 2018; Banerjee 2018; Hamers et al. 2018; Leigh et al. 2018; Kremer et al. 2020; Ye et al. 2020; Stephan et al. 2019; Hoang et al. 2020; Wang et al. 2020; Rastello et al. 2021; Fragione 2021). Furthermore, it was suggested that AGN disks may assist with the merger of BH binaries (Bartos et al. 2017; Stone et al. 2017, e.g.,).

(3) Secular evolution in hierarchical triple systems. This channel considers the long term evolution of triple body system via the Eccentric Kozai-Lidov (EKL) mechanism (e.g., Lidov 1962; Kozai 1962; Naoz 2016, see latter for review).

The EKL mechanism drive the inner binary to high eccentricity, which boost the GW emission power of the inner binary and lead to a merger. Triples are hosted either in the field of the host galaxy (Antonini et al. 2016, 2017; Silsbee & Tremaine 2017; Liu & Lai 2018; Vigna-Gómez et al. 2021, e.g.,) or in dense environments (Britt et al. 2021; Miller & Hamilton 2002; Antonini et al. 2014; Kimpson et al. 2016; Samsing et al. 2018; Hamilton & Rafikov 2019; Martinez et al. 2020, e.g.,). Moreover, at the center of galaxies, the third object can be the supermassive BH (e.g., Antonini & Perets 2012; Stephan et al. 2016, 2019; Petrovich & Antonini 2017; Hoang et al. 2018; Fragione et al. 2019; Wang et al. 2020).

(4) Mergers from ultra wide systems in the field. Recently, it was shown that isolated ultra-wide systems (with semi-major axis (SMA) $> 100\text{AU}$), either binaries or triples, in the field of the host galaxy, may be driven to extremely high eccentricities to allow strong interaction between the two binary objects (Michaely & Perets 2016, 2019; Michaely & Perets 2020; Michaely 2020; Michaely & Shara 2021). For ultra-wide systems, the field is collisional environment due to consecutive frequent flyby interactions with random field stars. These interactions may excite the eccentricity (in the case of binaries) or outer eccentricity (in case of triples), with the result that mergers can occur via increased GW emission (binaries) or three-body instabilities (triples).

Here we focus on this latter channel and study the BHNS formation channel. In particular we present a novel scenario that can lead to a BHNS merger via GW and a possibility to a EM counterpart.

In the last years the majority of the literature focused on the BBH formation channels. However, recently a few studies have focused on identifying the possible origins of these BHNS mergers, (e.g., Hoang et al. 2020; Ye et al. 2020; Mandel & Smith 2021, see former study's introduction for an overview of the field).

BHNS mergers are uniquely interesting due to the possibility of an electromagnetic (EM) counterpart signal caused by the disruption of the NS from the BH tidal forces. This might result in a short-Gamma ray burst (sGRB, e.g., Berger 2014) and other EM transients. sGRBs are intense, non-repeating and short flashes of gamma rays caused by the disruption of a NS due to tidal forces from its companion (either a NS or a BH, in this manuscript we focus on the BH-NS binaries). Unlike, long duration GRBs (longer than 2 seconds), which are associated with massive stars or core-collapse supernovae, that are observed solely in star forming galaxies, sGRBs are observed in both, star forming galaxies and elliptical galaxies. Overall about 20% of sGRBs are found in early-type (elliptical and $S0$ galaxies) (e.g., Leibler & Berger 2010; Berger 2014). Here we show that our novel channel naturally predicts $\sim 1\% - 50\%$ of all BH-NS mergers to be accompanied with sGRB transient.

This paper is organized as follows. In section 2 we preset the physical picture, derive the governing rate equations and calculate the merger rates. We discuss the results and summarize the manuscript in section 3.

2. PHYSICAL PICTURE

2.1. *The Collisional Nature of Ultra-Wide Binaries in the Field*

This section describes the merger scenario and calculates the merger rate for a Milky-Way (MW)-like galaxy and an elliptical galaxy. Although low in stellar density, the galactic field is considered collisional for ultra-wide systems. These wide systems interact relatively frequently with random flyby stars in the field because of their large interaction cross-section proportional to their SMA. Hence, an ultra-wide system encounters many random interactions with flyby field stars.

These interactions are typically impulsive by nature, i.e., the interaction timescale $t_{\text{int}} \equiv b/v_{\text{enc}}$ (where b denotes the closest approach to the binary's center of mass, and v_{enc} denotes the relative velocity between the random flyby star and the binary) is much shorter than the orbital period time, P . Moreover, these interactions change the binary orbit characteristics, namely the orbital energy (decrease/increase the SMA), but more significantly, torque the system and change the binary eccentricity e (e.g., Lightman & Shapiro 1977; Merritt 2013). After many impulsive interactions the wide binary might be driven into a sufficiently high eccentricity, and as a result to sufficiently small pericenter distance, q , which allows the binary to merge via GW emission within Hubble time (or less). Once a BH-NS mergers

via GW we might expect an EM transient associated with the mergers, namely a sGRB.

2.2. Relevant Timescales

As mentioned above in this scenario, the impulse interaction timescale $t_{\text{int}} \equiv b/v_{\text{enc}}$ needed to be shorter than the binary orbital period P . Specifically we require that $t_{\text{int}} = \alpha P$, with $\alpha \ll 1$. This gives upper bound to the closest approach distance, $b_{\text{impulse}} = \alpha P v_{\text{enc}}$ and hence limits the average time between encounters. For example, consider a binary with total mass of $10M_{\odot} + 1.5M_{\odot} = 11.5M_{\odot}$, SMA of $a \sim 10^4 \text{AU}$ which translates to an orbital period of $P \approx 3.2 \times 10^5 \text{yr}$ and velocity encounter of $v_{\text{enc}} = 50 \text{kms}^{-1}$ we can restrict b_{impulse} for $\alpha = 0.1$. Thus, we get $b_{\text{impulse}} = \alpha t_{\text{int}} \times v_{\text{enc}} \sim 3.3 \times 10^5 \text{AU}$.

Additionally, we consider the average time between two flybys of the binary system and a random stellar perturber, $t_{\text{enc}} = 1/f = (n_* \sigma v_{\text{enc}})^{-1}$ where n_* denotes the stellar number density, $\sigma = \pi b^2$ is the geometric cross-section of the binary and the stellar fly-by, and v_{enc} is the relative velocity of the fly-by and the binary center of mass.

Lastly, we consider the GW timescale (e.g., Peters 1964)

$$t_{\text{merger}} \approx \frac{a^4}{\beta'} \times (1 - e^2)^{7/2} \quad (1)$$

where

$$\beta' = \frac{85}{3} \frac{G^3 m_{\text{BH}} m_{\text{NS}} (m_{\text{BH}} + m_{\text{NS}})}{c^5}$$

G is Newton's constant and c is the speed of light. Thus, we focus on the merger of a wide binary with semi-major axis, $a > 10^2 \text{AU}$.

2.3. Analytic Description of the BH-NS merger

Consider an ensemble of isotropic wide binaries, each consisting of a BH with mass $m_{\text{BH}} = 10$ and a NS with mass $m_{\text{NS}} = 1.5M_{\odot}$. We assume all binaries to have the same SMA, and a thermal distribution of orbital eccentricities, $f(e)de = 2ede$. We derive the merger probability from this ensemble and find its dependence on the SMA of the binaries, a for a given environment, i.e. stellar density n_* and velocity dispersion.

We start by calculating the fraction of system that merge from this ensemble given thermal distribution of eccentricity using Equation (1).

Given the merger time $t_{\text{merger}} = T$ and the SMA of the binary a we define a critical eccentricity e_c

$$e_c = \left[1 - \left(\frac{\beta' T}{a^4} \right)^{2/7} \right]^{1/2}, \quad (2)$$

for which all systems with eccentricities equal or greater than e_c merge within time T . Below we will adopt T as the average encounter time. Thus, given a thermal distribution of eccentricities we find the fraction of systems that merger within T and lost from the ensemble to be:

$$F_q = \int_{e_c}^1 2ede = 1 - e_c^2 = \left(\frac{\beta' T}{a^4} \right)^{2/7}. \quad (3)$$

All other binaries outside the loss-cone are susceptible for interaction with a random flyby and can be perturbed to change their angular momentum and replenish the loss cone.

After a single random flyby interaction the relative velocity vector of the binary changes. The new direction of the velocity vector maps a cone around the original relative velocity vector. The average *fraction* of the phase-space region into which the binaries in the ensemble are perturbed after a single fly-by is termed the smear cone. The smear cone is computed by the ratio of the size of the cone with all possible directions (e.g., Kaib & Raymond 2014; Michaely & Perets 2016, 2019). In order to calculate the smear cone one should first find the size of which, and defined by the following:

$$\theta = \frac{\langle \Delta v \rangle}{v_k}, \quad (4)$$

where v_k is the Keplerian velocity of the binary and $\langle \Delta v \rangle$ is the average change of v_k from a single perturbation. The value of v_k is calculated at the average separation of a Keplerian orbit is $\langle r \rangle = a(1 + 1/2e^2)$ and we approximate $e \rightarrow 1$, yielding

$$v_k \sim \left(\frac{GM}{3a} \right)^{1/2},$$

where $M \equiv (m_{\text{BH}} + m_{\text{NS}})$ is the total mass of the binary.

The average change of the Keplerian velocity, $\langle \Delta v \rangle$ is given by (e.g., Hills 1981)

$$\langle \Delta v \rangle \simeq \frac{3G a m_p}{v_{\text{enc}} b^2}, \quad (5)$$

where v_{enc} is the velocity of the fly-by star with respect to the binary center of mass, m_p is the perturber mass. Therefore, the square of the angular size of the smear cone cause by the impulse of the fly-by on the binary is (using Equations (4) - (5))

$$\theta^2 = \frac{9G^2 a^2 m_p^2}{(v_{\text{enc}} b^2)^2} \frac{3a}{GM} = \frac{27G a^3 m_p^2}{M (v_{\text{enc}} b^2)^2}, \quad (6)$$

and for $\theta \ll 1$ we get the average size of the cone post interaction. The smear-cone is the fraction of that size with all possible directions, i.e. over the 4π sphere to

be after a single passage of the perturber (e.g., [Kaib & Raymond 2014](#); [Michaely & Perets 2016, 2019](#))

$$F_s = \frac{\pi\theta^2}{4\pi} = \frac{27}{4} \left(\frac{m_p}{M}\right)^2 \left(\frac{GM}{av_{\text{enc}}^2}\right) \left(\frac{a}{b}\right)^4. \quad (7)$$

For a given binary, the smear cone size in Equation (7) depends on the perturber and the environment, specifically, its mass, m_p , closest approach, b and the encounter velocity, v_{enc} .

The ratio between the smear and loss cones, is the fraction of the loss cone filled after a single flyby. Namely, for cases where $F_s \geq F_q$ the entire ensemble regain its thermal eccentricity distribution.

$$\frac{F_s}{F_q} = \frac{27}{4} \left(\frac{m_p}{M}\right)^2 \left(\frac{GM}{av_{\text{enc}}^2}\right) \left(\frac{a}{b}\right)^4 \left(\frac{a^4}{\beta'T}\right)^{2/7}. \quad (8)$$

The are two conditions for the loss cone to be continuously full is (1) that the kick is sufficiently strong to fill the loss cone, namely, $F_s \geq F_q$, and (2) the replenishment is as fast as the orbits are lost from the ensemble. The replenishment rate is determined by the interaction rate which can easily be calculate by

$$f \equiv \frac{1}{t_{\text{enc}}} = n_* \sigma(b) v_{\text{enc}}. \quad (9)$$

The first condition, the demand that the flyby kick is sufficiently strong, sets a limit on the closest approach,

$$b_{\text{kick}}^2 \leq v_{\text{enc}}^{-1} \left(\frac{27G}{4} a^{29/7} \frac{m_p^2}{M} \left(\frac{n_* \pi}{\beta'T}\right)^{2/7}\right)^{7/12}. \quad (10)$$

We set the close approach to be the minimum of the two distance scales, the first b_{impulse} is required because we focus only on the impulsive regime, the second b_{kick} is required to ensure each fly-by is sufficiently strong to fill the loss cone. Specifically,

$$b = \min(b_{\text{kick}}, b_{\text{impulse}}), \quad (11)$$

see Figure 1 for visualization.

Next, we can calculate the average encounter time, t_{enc} from Equation (9). We chose the merger time to the average time between encounters, which is a function of the closest approach, $T \equiv t_{\text{enc}}(b)$. Note that the merger time T is dependent on the closest approach b , which is determined from Equation (11).

Now we are set to find the critical SMA from which the loss cone is continuously full, under the impulse approximation, as a function of the local environment characteristics. Thus, for $F_s = F_q$ and $1/t_{\text{enc}} = n_* \sigma v_{\text{enc}}$, we find:

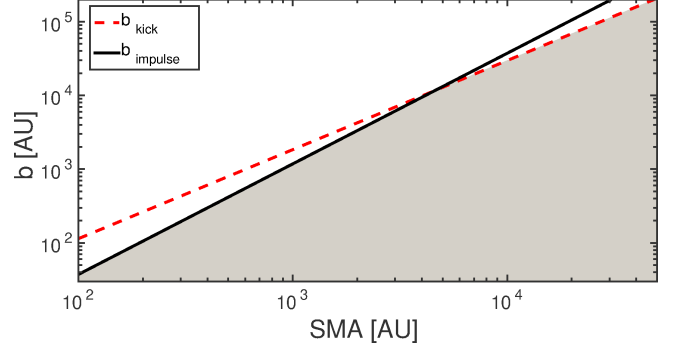


Figure 1. The two distance scales b_{kick} (dashed red) and b_{impulse} (solid black). Each fly-by with $b < b_{\text{kick}}$ will fill the loss cone and each one with $b < b_{\text{impulse}}$ will interact impulsively with the wide BHNS binary. We are interested in the grey area which insures both conditions. Calculated for binary with $m_{\text{BH}} = 10M_{\odot}$ and $m_{\text{NS}} = 1.5$ with $v_{\text{enc}} = 60\text{kms}^{-1}$. The stellar density number is $n_* = 0.1\text{pc}^{-3}$.

$$a_{\text{crit}} = \left[\frac{4}{27} \frac{M \beta'^{2/7} T(b)^{-12/7}}{G m_p^2 n_*^2 \pi^2} \right]^{7/29}. \quad (12)$$

Another way to express the critical SMA is without the specific explicit function of the geometric cross section, σ

$$a_{\text{crit}} = \left(\frac{GM}{n_*^2 \sigma(b)^2 v_{\text{enc}}^2} \right)^{1/3}. \quad (13)$$

Binaries with SMA than equal to the a_{crit} have the highest probability to merger via GW emmision. Binaries with SMA smaller than a_{crit} are harder to perturb, therefore the probability rate decreases. Binaries with SMA larger than a_{crit} also descreas in probability due to the smaller loss cone, additionally, these binaries are more likely to become unbind during the interaction, e.g. [Michaely & Perets \(2019\)](#). This interplay leads to a sharp transition in the merger probability, as highlighted in Figure 2, see below.

In other words, the full loss cone regime is for all systems with $a > a_{\text{crit}}$. The loss rate of systems from the full loss-cone, (\dot{L}_{full}), is given by the rate they leave the loss cone

$$\dot{L}_{\text{full}} = \frac{F_q}{P}. \quad (14)$$

On the other hand, tighter binaries are less susceptible for change due to a fly-by, this is evident from equation (7). Therefore for $a < a_{\text{crit}}$ we expect that the loss cone will not be full all the time, in this “empty loss cone” the loss rate depends on the rate of orbits being kicked into the loss cone is just the interaction rate, f :

$$\dot{L}_{\text{empty}} = F_q f = \frac{F_q}{t_{\text{enc}}} \quad (15)$$

From the critical SMA we can calculate the merger probability for each regime, for $a < a_{\text{crit}}$ (empty loss cone) and for $a > a_{\text{crit}}$ (full loss cone). We note here that by considering the critical SMA we implicitly include the dependency on the impact parameter, b .

In what follows we calculate the time dependent loss probability of the two regimes, the empty and full cones. We note that F_q is the fraction of systems that are lost from the ensemble and therefore $(1 - F_q)$ represents the fraction of binaries that survive as wide binaries at the relevant timescale, after a single flyby with the relevant timescale. Therefore, $(1 - F_q)$ is a monotonically decreasing function of time. Hence, the surviving fraction of binaries after time t and the relevant timescale for the empty loss cone f is $(1 - F_q)^{tf}$ (e.g., Kaib & Raymond 2014; Michaely & Perets 2016, 2019). Therefore the probability for a wide binary merger, which complements this expression to unity is

$$L_{a < a_{\text{crit}}} = 1 - (1 - F_q)^{tf} \quad (16)$$

where t is the time since birth of the binary. As one can expect the probability only depends on the size of the loss cone and the rate of interactions. For the limit of $tfF_q \ll 1$ we can expand Equation (16) and take the leading term, to find the loss probability to be approximated by

$$L_{a < a_{\text{crit}}} = tf(b)F_q. \quad (17)$$

For the full loss cone regime the limiting factor is not the value of f , but rather the orbital period P . Therefore, the full expression for the loss probability for $a > a_{\text{crit}}$ is

$$L_{a > a_{\text{crit}}} = 1 - (1 - F_q)^{t/P}. \quad (18)$$

For the limit $F_q \cdot t/P \ll 1$ we can approximate the probability by

$$L_{a > a_{\text{crit}}} = tF_q \frac{1}{P(a)}. \quad (19)$$

Until this point we neglect the "ionization" of wide binaries in the field. This process reduce the available number of wide binaries. To account for this we use the half-life time approximate relation given by (Bahcall et al. 1985), the half-life time of a wide binary is

$$t_{1/2} = 0.00233 \frac{v_{\text{enc}}}{Gm_p n_* a}. \quad (20)$$

Correcting for this we get for Equation (17) and Equation (19) the following approximations:

$$L_{a < a_{\text{crit}}} = \tau f(b)F_q \left(1 - e^{-t/\tau}\right) \quad (21)$$

and

$$L_{a > a_{\text{crit}}} = \tau \frac{F_q}{P(a)} \left(1 - e^{-t/\tau}\right), \quad (22)$$

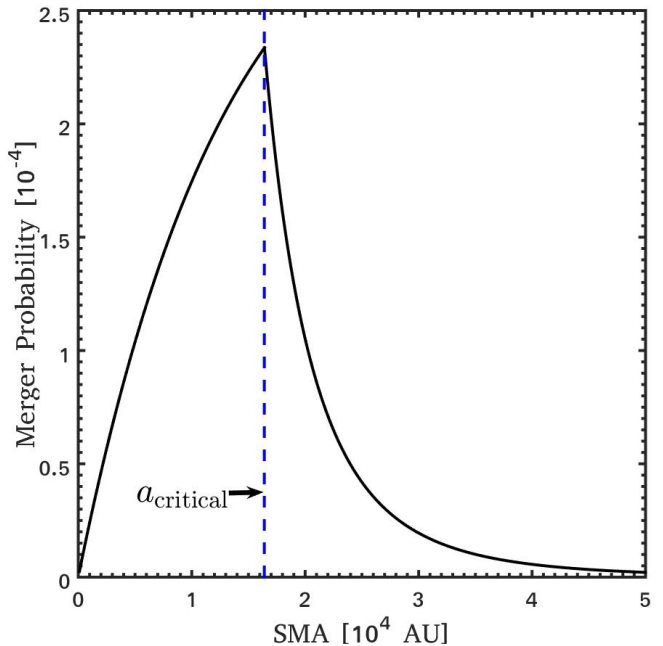


Figure 2. The merger probability of BHNS with $m_{\text{BH}} = 10M_{\odot}$ and $m_{\text{NS}} = 1.5$ with fly-by mass $m_p = 0.6M_{\odot}$ and $v_{\text{enc}} = 50\text{kms}^{-1}$. The stellar density number is $n_* = 0.1\text{pc}^{-3}$. The probability is calculated after $t = 10\text{Gyr}$ since the BHNS was formed. The peak probability is achieved at $a = a_{\text{crit}}$. For binaries with tighter orbits the merger probability drops because it is harder to change their orbital parameters. For binaries with $a > a_{\text{crit}}$ the probability decreases because the loss cone dependency with a , see text.

where $\tau = t_{1/2}/\ln 2$ is the mean lifetime of the binary. For a more detailed derivation see equations (11) and (12) in Michaely & Perets (2019) and in the Appendix.

2.4. Volumetric merger rates

In this subsection we calculate the GW signal rate of the local universe from wide BH-NS binaries. In order to do that we need (1) to approximate the fraction of wide BH-NS binaries out of the stellar population. (2) To model the stellar density of the host galaxy.

First we estimate the fraction of wide BH-NS systems from the stellar population. The initial binary is comprised out of two stars with masses M_1 and M_2 . As a prove of concept we assume that all stars with zero age main sequence (ZAMS) masses greater than $20M_{\odot}$ turn into BHs without any natal-kicks (Belczynski et al. 2016; Mandel 2016, and others). We emphasize that this is a simplifying assumption, it is currently unknown the mapping of ZAMS, metallicity and the stellar spin to the remnant BH mass. Additionally, we assume that all stars with ZAMS between $8 - 10M_{\odot}$ turn into NS via electron capture Supernova (SN) and born without natal kicks (Nomoto 1982, 1984). For

Kroupa (Salpeter) initial mass function (IMF) we find that $f_{\text{BH}} \approx 2 \times 10^{-3}$ (5×10^{-4}) (Kroupa 2001; Salpeter 1955). The companion mass is calculated given a mass ratio distribution, $Q \equiv M_2/M_1$ with $Q \propto M_1^{-2}$ (Moe & Di Stefano 2016) with the boundaries $Q_{\text{outer}} \in (0.3, 1)$, this translate to $f_{\text{NS}} \approx 0.13$ (0.12). We assume that the binary fraction $f_{\text{binary}} = 1$ (Duchêne & Kraus 2013). Next we estimate the fraction of binaries with SMA greater than $a > 1000\text{AU}$ to be $f_{\text{wide}} \approx 0.2$ (Michaely & Perets 2019)

$$f_{\text{BH-NS}} = f_{\text{BH}} \times f_{\text{NS}} \times f_{\text{binary}} \times f_{\text{wide}} \approx 5.2 \times 10^{-5} \quad (23)$$

and for Salpeter IMF we get $f_{\text{BH-NS}} \approx 1.2 \times 10^{-5}$.

Next, we model the stellar density function for a Milky-Way like spiral galaxy and for an elliptical galaxy. For the spiral case we follow the model used in (Michaely & Perets 2016). The number of stars in region dr at a distance r from the center is

$$dN(r) = n_*(r) 2\pi r h dr \quad (24)$$

where the scale height is h . We continue with modeling the Galactic stellar density in the Galactic disk as follows

$$n_*(r) = n_0 e^{-(r-r_\odot)/R_l}, \quad (25)$$

where $n_0 = 0.1\text{pc}^{-3}$ is the stellar density in the solar neighborhood, $R_l = 2.6\text{kpc}$ (Jurić et al. 2008) is the galactic length scale and $r_\odot = 8\text{kpc}$ is the distance of the Sun from the Galactic center. The mass of the perturber is taken to be $0.6M_\odot$ which is the average mass of a star in the galaxy. The encounter velocity is set to be the velocity dispersion of the flat rotation curve of the galaxy, namely $\hat{\sigma} = 50\text{kms}^{-1}$.

For the elliptical galaxies, we use the density profile function from (Hernquist 1990), given the average stellar mass of $0.6M_\odot$ we get

$$\tilde{n}_*(r) = \frac{M_{\text{galaxy}}}{2\pi r} \frac{r_*}{(r + r_*)^3} \quad (26)$$

where $r_* = 1\text{kpc}$ is the scale length of the galaxy, $M_{\text{galaxy}} = 10^{11}M_\odot$ is the total stellar (not including dark matter) mass of the galaxy, we focus on $r = 0.5 - 30\text{kpc}$. The elliptical galaxy velocity dispersion is taken to be $\hat{\sigma} = 160\text{kms}^{-1}$.

The merger rate is calculated by integrating the merger probability for all SMA, with log-uniform distribution, f_a , and the entire host galaxy

$$\Gamma_{\text{MW}} = \int_{0.5\text{kpc}}^{15\text{kpc}} \int_{100\text{AU}}^{5 \cdot 10^4\text{AU}} \frac{L(a, r)}{T_{\text{int}}} f_a f_{\text{BH-NS}} da dr \quad (27)$$

where T_{int} is the integration time, for $T_{\text{int}} = 10\text{Gyr}$ the average merger rate, Γ is for the lifetime of the host

galaxy. The integral limits are taken to be the relevant size of the MW galaxy and the all the binaries SMA we consider. The function $L(a, r)$ is taken from eq. (21) and (22). Thus, for the MW-like galaxy we get

$$\Gamma_{\text{MW}} \approx 0.06\text{Myr}^{-1}, \quad (28)$$

where, we use Belczynski et al. (2016) in order to calculate the merger rate, R per Gpc^3 by using the following equation

$$R_{\text{MW}} = 10^3 \rho_{\text{gal}} \times \Gamma_{\text{MW}} \approx 0.66\text{Gpc}^{-3}\text{yr}^{-1} \quad (29)$$

while ρ_{gal} is local density of the MW-like galaxies with the value of $\rho_{\text{gal}} = 0.0116\text{Mpc}^{-3}$ (e.g. Kopparapu et al. (2008)) and Γ_{MW} is given in the units of Myr^{-1} .

For the elliptical case we compute:

$$\Gamma_{\text{elliptical}} = \int_{0.5\text{kpc}}^{30\text{kpc}} \int_{100\text{AU}}^{5 \cdot 10^4\text{AU}} \frac{L(a, r)}{T_{\text{int}}} f_a f_{\text{BHNS}} da dr \quad (30)$$

and get $\Gamma_{\text{elliptical}} \approx 0.39\text{Myr}^{-1}$.

The number density of elliptical galaxies in the local universe elliptical is crudely approximated by $\sim 0.1\text{Mpc}^{-3}$ (Samsing et al. 2014) and get

$$R_{\text{elliptical}} \approx 39\text{Gpc}^{-3}\text{yr}^{-1}. \quad (31)$$

Adding the contributions of each type of galaxy, we get

$$R_{\text{tot}} = R_{\text{elliptical}} + R_{\text{MW}} \approx 40\text{Gpc}^{-3}\text{yr}^{-1}. \quad (32)$$

3. DISCUSSION AND SUMMARY

3.1. Caveats and assumptions

The mathematical model we present here is simplistic and based on several assumptions.

BH masses: As mentioned in Sec. 2.4, we make simplifying assumptions on the remnant mass of the BH. The mapping of initial mass of the star, metallicity and spin to final BH mass is not well understood. The stellar evolution physics, e.g. wind mass loss, nuclear physics and supernova physics (Baes et al. 2007; Zhu et al. 2010; Fryer et al. 2012). Hence we present our results with the prefactor of $f_{\text{BH}} = 2 \times 10^{-3}$. Different assumption will lead to different fraction of BH from the initial populations.

BH Natal kicks: The calculated merger rates depends strongly on the binary fraction estimation. This estimation is stringently depended on the natal kicks upon formation of BHs. These natal kicks are poorly constrained (e.g., Repetto et al. 2012, 2017). However, there are evidence that BH are formed by failed SN (e.g., Ertl et al. 2015). In the failed SN scenario large amount of fallback is accreted on the newly formed compact object

and suppresses any natal kicks. Moreover, many theoretical studies of GW merger rate assume not natal-kicks for BH (e.g., Belczynski et al. 2007, 2008, 2016).

NS Natal kicks: From the observations of pulsar it is well known that NS are born with natal kicks. However, in the narrow range of masses between $8 - 10M_{\odot}$, stars are believed to undergo e-electron capture SN. In this work we limit ourselves only to this narrow range of stars and assume no natal kicks for the newly born NS.

SMA and eccentricity distributions The underlying assumption of the results presented here are the distributions of the SMA and eccentricities of the wide systems. We use Opik law, namely, log-uniform distribution for the SMA of the systems, and use thermal eccentricity distribution for the eccentricity of the binaries.

3.2. Model Predictions and Signatures

In this study we explore a novel scenario that may lead to a merger between BH and a NS or a NS disruption. In what follows we present some of the model features.

3.2.1. Velocity dispersion

A unique signature of the model presented here is the dependence on the host galaxy velocity dispersion. The velocity dispersion sets the rate of encounters and the timescale of binary ionization. Following the model presented in the previous section we can calculate the scaling relation between the merger rate and the host galaxy velocity dispersion. We distinguish between the regime where $b = b_{\text{kick}}$ and the regime where $b = b_{\text{impulsive}}$. For simplicity we start with the non-ionized case Equation (17) and Equation (19). The scaling relation is calculated by considering each term dependency on v_{enc} . The frequency $f \propto v_{\text{enc}}$ from equation (9). The loss cone, $F_q \propto T^{2/7} a^{-8/7}$, noting that $a \propto v_{\text{enc}}^{-2/3}$ from equation (13) we get $F_q \propto v_{\text{enc}}^{10/21}$. Therefore we get:

$$L_{\text{impulse,empty}} = t f F_q \propto v_{\text{enc}}^{31/21} \quad (33)$$

The integrated rate, Γ , is the integral of (33) over all SMA, $\int L f_a da$. Hence, the scaling relation is

$$\Gamma \propto L \frac{1}{a_{\text{crit}}} a_{\text{crit}} \propto v_{\text{enc}}^{31/21} \quad (34)$$

Including the ionization process, the merger probability changes to Eq. (21), where

$$\tau \propto \frac{v_{\text{enc}}}{a}. \quad (35)$$

For the case of $-t/\tau \rightarrow 0$ we get $\tau \propto v_{\text{enc}}^0$ for the other extreme, $-t/\tau \rightarrow \infty$ we get $\tau \propto v_{\text{enc}}^{5/3}$. For the regime where $b = b_{\text{kick}}$, the calculation is similar but with different scaling. Specifically,

$$L_{\text{kick,empty}} = t f F_q \propto v_{\text{enc}}^0. \quad (36)$$

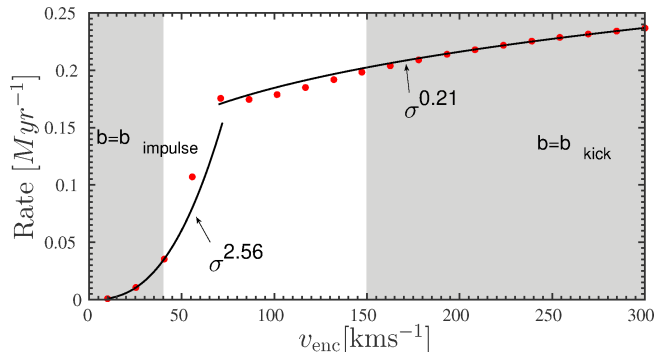


Figure 3. Average merger rate for a MW galaxy-like as a function of unrealistic velocity dispersion. Rate is calculated after 10^{10} yrs from star formation accounting for binary ionization. Binaries consist of $m_{\text{NS}} = 1.5M_{\odot}$ and $m_{\text{BH}} = 10M_{\odot}$. For $v_{\text{enc}} \lesssim 40$ ($\gtrsim 150$) kms^{-1} , the closest approach $b = b_{\text{impulsive}}$ ($b = b_{\text{kick}}$) for all SMA (grey area), see text. The white area is a mix of both regimes. The rate for an elliptical galaxy shows a similar behavior and is omitted here to avoid clutter.

As a result the v_{enc} dependency disappears in the non-ionization case. Once we include ionization we get the following:

$$\Gamma \propto \int \tau L f_a da (1 - e^{-t/\tau}) \propto v_{\text{enc}} (1 - e^{-t/\tau}), \quad (37)$$

where

$$\tau \propto v_{\text{enc}}. \quad (38)$$

In Figure 3 we depict the merger rate scaling relation as a function of the velocity encounter for a range of velocity dispersions. One can see the crossover in scaling around $v_{\text{enc}} \approx 70 \text{ km s}^{-1}$ between the impulsive and the kick regimes.

Currently we cannot identify BHNS mergers for a specific galaxy, however, it is possible to assign a host galaxy to a sGRB coincident with GW detection.

3.2.2. Delay time distribution

The BHNS delay time distribution (DTD), $d\Gamma/dt$, is the binary merger rate as a function of time since star formation. In this case we ignore the stellar evolution time, which is much quicker ($\sim 10^6$ yr) than galaxy lifetime timescale ($\sim 10^{10}$ yr). One can calculate the expected DTD of GW sources, Γ , from this channel numerically, specifically we compute equations (27) and (30) for different integration times, T_{int} . If we ignore the ionization process, we expect a constant DTD, because the merger probability from equations (17) and (19) are linear in t . However, in reality wide systems are continuously ionized in the field due to the flyby interactions, and there are less available binaries to merger via GW. The time dependence is given by Equations (21) and

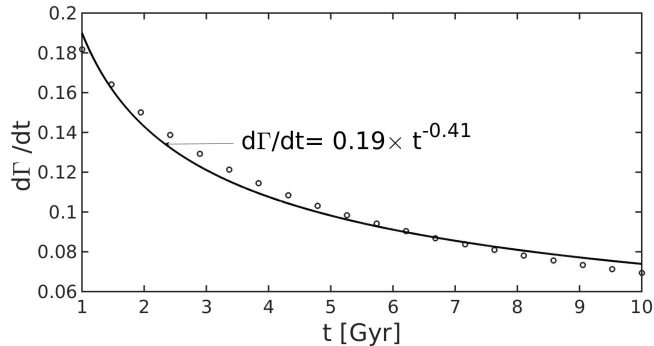


Figure 4. The Delay time distribution (DTD) for a MW-like galaxy with velocity dispersion of $\sigma = 40\text{kms}^{-1}$. Blue circles are the model calculations. Black solid line is the best power law fit. Note that this fit is specific for MW-galaxy adopted here, see text for more details. The GW merger span for the entire lifetime of the galaxy, which suggests these mergers occur in early and late type of galaxies.

(22). We solve these equations numerically for different times after formation. We note that the total rate also depends on the SMA and local stellar density, which make the analytical dependence of t very complicated, therefore we only find the DTD numerically. In Figure 4 we present the DTD for MW-like galaxy, we present the best power law fit in order to compare to the classical $1/t$ we expect from SNe (Maoz et al. 2014) and sGRB (Berger 2014). We find for a MW-like galaxy the DTD is proportional to $\sim t^{-0.41}$. The exact value of the power law depends on the host galaxy characteristics (velocity dispersion and the distribution of the stellar density), as well as the distribution of the SMA of the wide binaries.

3.2.3. Mass ratio

Here we present the model dependency on the mass ratio, $Q \equiv m_{\text{NS}}/m_{\text{BH}}$. Unlike Michaely & Perets (2019) that considered BBH, here one of the companions is a NS and therefore has a constant mass. It is important to note that the merger rate dependency on Q might be a source of confusion. In our case, NS-BH binary, a change in Q infers also a change in the total binary mass M , due to the constant NS mass. Moreover, in what follows we do not assume the BH mass distribution but rather just present the merger rate assuming all BHs have the same mass. In Figure 5 we present the merger rate as a function of mass ratio Q . We find that for the BHNS case a higher merger rate for lower Q , as can be seen in Figure 5.

3.2.4. Spin distribution

Because the origin of these mergers are from extremely wide binaries we do not expect these compact objects to have any correlation in their respective spins. Therefore, one should not expect any spin alignment between the

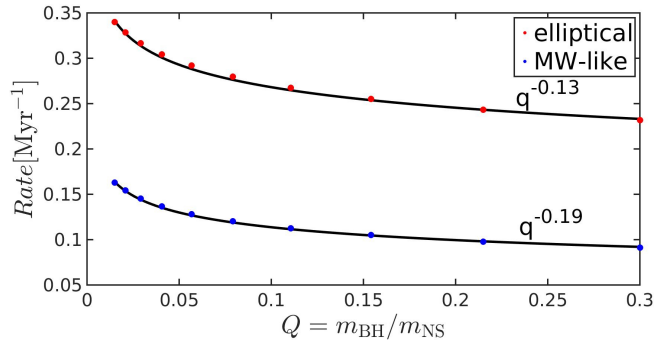


Figure 5. Average merger rate for a MW galaxy-like (red dots) and elliptical galaxy (blue dots). The velocity dispersion is $\sigma = 40\text{kms}^{-1}$ for the MW-like galaxy and $\sigma = 160\text{kms}^{-1}$ for the elliptical. Rate is calculated after 10^{10} yrs from star formation, for binaries with $m_{\text{NS}} = 1.5M_{\odot}$ and varying $m_{\text{BH}} = 10M_{\odot}$.

BH and the NS in the moment of merger. Similar to other dynamically induced mergers the ξ_{eff} is expected to be close to zero.

3.3. sGRB

Any BHNS merger is a potential for sGRB (Berger 2014). A merger will not result in a disruption of the NS if the NS enters the BH event horizon in its entirety and therefore EM radiation is not created and omitted. The physical quantity that governs the outcome of the merger, whether or not it will produce an EM transient is the NS equation of state (EOS) which is still unconstrained. Fragione (2021) showed that for the fraction of BH-NS mergers that produce a sGRB, under some assumptions of their EOS is $\sim 1 - 50\%$. Accounting for this fraction and our merger rates we get that the sGRB from R_{tot} :

$$\Gamma_{\text{sGRB}} \approx 0.5 - 20\text{Gpc}^3\text{yr}^{-1}. \quad (39)$$

Additionally, unlike GW mergers detection, which we have very poor localization, and currently cannot assign a host galaxy to the detection, we are able in principle to identify the host galaxy, and check this model assumptions. For example, as mentioned above, sGRB are observed in both star forming galaxies and in ellipticals. This can be explained when considering the DTD of this model, see Figure 4. The DTD extends from star formation till 10^{10} yr, thus we expect these mergers and sGRBs to in both star forming and elliptical galaxies.

3.4. Summary

In this paper we present a novel dynamical channel for the formation of field wide BH-NS binaries mergers via GWs by random flyby interactions with passing stars. We find that the volumetric merger rate is up

to $R_{\text{tot}} \approx 40\text{Gpc}^3\text{yr}^{-1}$. Additionally, we report the following signatures: (1) the merger rate increase with the host galaxy velocity dispersion.

(2) The DTD is function of the galaxy characteristics and shallower than uniform but steeper than $1/t$. For a MW-like spiral galaxy is $\propto t^{-0.41}$.

(3) The merger rate decrease with increasing mass ratio of the binary.

(4) The effective spin distribution is expected to be zero due to the fact that the merger is originating from initially wide binary system, which we do not expect to have any correlations in a the spins.

(5) EM radiation, in the form of sGRB is expected to occur from 1 – 50% of the merger we calculate, which translates in for this scenario up to $0.4 - 20\text{Gpc}^3\text{yr}^{-1}$.

ACKNOWLEDGMENTS

EM and SN thank the Bhaumik Institute for Theoretical Physics and Howard and Astrid Preston for their generous support. We also acknowledges the partial support from NASA ATP 80NSSC20K0505.

APPENDIX

Here we present the explicit function form of the rate equation. We distinguish between two different regimes, the impulsive regime and the kick regime.

Impulsive regime. In this case $b_{\text{impulsive}} < b_{\text{kick}}$. We remind the reader that $b_{\text{impulsive}} = \alpha P v_{\text{enc}}$, hence the explicit form of the critical SMA is

$$a_{\text{crit}} = \left(\frac{(GM)^{3/2}}{8\pi^4 n_* v_{\text{enc}}^3 \alpha^2} \right)^{2/9} \quad (1)$$

and the corresponding f is

$$f(a) = n_* \alpha^2 P(a)^2 v_{\text{enc}}^3 = n_* \alpha^2 \left(\frac{4\pi^2 a^3}{GM} \right) v_{\text{enc}}^3. \quad (2)$$

The loss cone F_q is given by (3), hence the loss rate function for the impulsive regime, without accounting for binary ionization, is given by the following two equations, the first for the empty loss cone regime:

$$L_{a < a_{\text{crit}}} = t f F_q = t n_* \alpha^2 \left(\frac{4\pi^2 a^3}{GM} \right) v_{\text{enc}}^3 \left(\frac{\beta}{f(a) a^4} \right)^{2/7} \propto a \quad (3)$$

and for the full loss cone regime

$$L_{a > a_{\text{crit}}} = t \frac{F_q}{P(a)} = t \left(\frac{\beta}{f(a) a^4} \right)^{2/7} \left(\frac{GM}{4\pi^2 a^3} \right) \propto a^{-5}. \quad (4)$$

However, in order to calculate the rate including the ionization that the binaries experience in the field one should take into account that half lifetime of the binaries from equation (20). This introduces a nontrivial dependency on the SMA, a and we get

$$L_{a < a_{\text{crit}}} = \tau f F_q (1 - e^{-t/\tau}) = \tau n_* \alpha^2 \left(\frac{4\pi^2 a^3}{GM} \right) v_{\text{enc}}^3 \left(\frac{\beta}{f(a) a^4} \right)^{2/7} (1 - e^{-t/\tau}) \quad (5)$$

and for the full loss cone

$$L_{a > a_{\text{crit}}} = \tau \frac{F_q}{P(a)} (1 - e^{-t/\tau}) = \tau \left(\frac{\beta}{f(a) a^4} \right)^{2/7} \left(\frac{GM}{4\pi^2 a^3} \right) (1 - e^{-t/\tau}). \quad (6)$$

Kick regime. In this case $b_{\text{impulsive}} > b_{\text{kick}}$. In this case b_{kick} is given by equation (10), and the corresponding a_{crit} and f are given by

$$a_{\text{crit}} = \left(\frac{GM}{n_* \pi^2} \right)^{6/47} \left(\frac{4M}{27Gm_p^2} \left(\frac{\beta}{n_* \pi} \right)^{2/7} \right)^{7/47} \quad (7)$$

and

$$f = n_* \sigma(b_{\text{kick}}) v_{\text{enc}} = n_* \pi \left(\frac{27G}{4} a^{29/7} \frac{m_p^2}{M} \left(\frac{n_* \pi}{\beta'} \right)^{2/7} \right)^{7/12}. \quad (8)$$

Next we write the rate equations for both the empty and full cone regimes, without binary ionization to get

$$L_{a < a_{\text{crit}}} = t f F_q = t n_* \pi \left(\frac{27G}{4} a^{29/7} \frac{m_p^2}{M} \left(\frac{n_* \pi}{\beta'} \right)^{2/7} \right)^{7/12} \left(\frac{\beta}{f(a) a^4} \right)^{2/7} \propto a^{7/12} \quad (9)$$

and

$$L_{a > a_{\text{crit}}} = t \frac{F_q}{P(a)} = t \left(\frac{\beta}{f(a) a^4} \right)^{2/7} \left(\frac{GM}{4\pi^2 a^3} \right) \propto a^{-29/6}. \quad (10)$$

Next we write the same rate equation with the correction for the binary ionization:

$$L_{a < a_{\text{crit}}} = \tau n_* \pi \left(\frac{27G}{4} a^{29/7} \frac{m_p^2}{M} \left(\frac{n_* \pi}{\beta'} \right)^{2/7} \right)^{7/12} \left(\frac{\beta}{f(a) a^4} \right)^{2/7} (1 - e^{-t/\tau}) \quad (11)$$

and

$$L_{a > a_{\text{crit}}} = t \frac{F_q}{P(a)} = \tau \left(\frac{\beta}{f(a) a^4} \right)^{2/7} \left(\frac{GM}{4\pi^2 a^3} \right) (1 - e^{-t/\tau}). \quad (12)$$

REFERENCES

- Antonini, F., Chatterjee, S., Rodriguez, C. L., et al. 2016, *ApJ*, 816, 65, doi: [10.3847/0004-637X/816/2/65](https://doi.org/10.3847/0004-637X/816/2/65)
- Antonini, F., Murray, N., & Mikkola, S. 2014, *ApJ*, 781, 45, doi: [10.1088/0004-637X/781/1/45](https://doi.org/10.1088/0004-637X/781/1/45)
- Antonini, F., & Perets, H. B. 2012, *ApJ*, 757, 27, doi: [10.1088/0004-637X/757/1/27](https://doi.org/10.1088/0004-637X/757/1/27)
- Antonini, F., Toonen, S., & Hamers, A. S. 2017, *ApJ*, 841, 77, doi: [10.3847/1538-4357/aa6f5e](https://doi.org/10.3847/1538-4357/aa6f5e)
- Baes, M., Sil'chenko, O. K., Moiseev, A. V., & Manakova, E. A. 2007, *A&A*, 467, 991, doi: [10.1051/0004-6361:20066758](https://doi.org/10.1051/0004-6361:20066758)
- Bahcall, J. N., Hut, P., & Tremaine, S. 1985, *ApJ*, 290, 15, doi: [10.1086/162953](https://doi.org/10.1086/162953)
- Banerjee, S. 2018, *MNRAS*, 473, 909, doi: [10.1093/mnras/stx2347](https://doi.org/10.1093/mnras/stx2347)
- Bartos, I., Haiman, Z., Marka, Z., et al. 2017, *Nature Communications*, 8, 831, doi: [10.1038/s41467-017-00851-7](https://doi.org/10.1038/s41467-017-00851-7)
- Belczynski, K., Kalogera, V., Rasio, F. A., et al. 2008, *ApJS*, 174, 223, doi: [10.1086/521026](https://doi.org/10.1086/521026)
- Belczynski, K., Repetto, S., Holz, D. E., et al. 2016, *ApJ*, 819, 108, doi: [10.3847/0004-637X/819/2/108](https://doi.org/10.3847/0004-637X/819/2/108)
- Belczynski, K., Taam, R. E., Kalogera, V., Rasio, F. A., & Bulik, T. 2007, *ApJ*, 662, 504, doi: [10.1086/513562](https://doi.org/10.1086/513562)
- Berger, E. 2014, *ARA&A*, 52, 43, doi: [10.1146/annurev-astro-081913-035926](https://doi.org/10.1146/annurev-astro-081913-035926)
- Britt, D., Johanson, B., Wood, L., Miller, M. C., & Michaely, E. 2021, *MNRAS*, 505, 3844, doi: [10.1093/mnras/stab1570](https://doi.org/10.1093/mnras/stab1570)
- de Mink, S. E., & Belczynski, K. 2015, *ApJ*, 814, 58, doi: [10.1088/0004-637X/814/1/58](https://doi.org/10.1088/0004-637X/814/1/58)
- de Mink, S. E., & Mandel, I. 2016, *MNRAS*, 460, 3545, doi: [10.1093/mnras/stw1219](https://doi.org/10.1093/mnras/stw1219)
- Dominik, M., Berti, E., O'Shaughnessy, R., et al. 2015, *ApJ*, 806, 263, doi: [10.1088/0004-637X/806/2/263](https://doi.org/10.1088/0004-637X/806/2/263)
- Duchêne, G., & Kraus, A. 2013, *ARA&A*, 51, 269, doi: [10.1146/annurev-astro-081710-102602](https://doi.org/10.1146/annurev-astro-081710-102602)
- Eldridge, J. J., Stanway, E. R., Xiao, L., et al. 2017, *PASA*, 34, e058, doi: [10.1017/pasa.2017.51](https://doi.org/10.1017/pasa.2017.51)
- Ertl, T., Janka, H.-T., Woosley, S. E., Sukhbold, T., & Ugliano, M. 2015, *ArXiv e-prints*. <https://arxiv.org/abs/1503.07522>
- Fragione, G. 2021, *ApJL*, 923, L2, doi: [10.3847/2041-8213/ac3bcd](https://doi.org/10.3847/2041-8213/ac3bcd)
- Fragione, G., Grishin, E., Leigh, N. W. C., Perets, H. B., & Perna, R. 2019, *MNRAS*, 488, 47, doi: [10.1093/mnras/stz1651](https://doi.org/10.1093/mnras/stz1651)
- Fragione, G., & Kocsis, B. 2018, *PhRvL*, 121, 161103, doi: [10.1103/PhysRevLett.121.161103](https://doi.org/10.1103/PhysRevLett.121.161103)
- Fryer, C. L., Belczynski, K., Wiktorowicz, G., et al. 2012, *ApJ*, 749, 91, doi: [10.1088/0004-637X/749/1/91](https://doi.org/10.1088/0004-637X/749/1/91)

- Gallegos-Garcia, M., Berry, C. P. L., Marchant, P., & Kalogera, V. 2021, *ApJ*, 922, 110, doi: [10.3847/1538-4357/ac2610](https://doi.org/10.3847/1538-4357/ac2610)
- Giacobbo, N., Mapelli, M., & Spera, M. 2018, *MNRAS*, 474, 2959, doi: [10.1093/mnras/stx2933](https://doi.org/10.1093/mnras/stx2933)
- Hamers, A. S., Bar-Or, B., Petrovich, C., & Antonini, F. 2018, *ApJ*, 865, 2, doi: [10.3847/1538-4357/aadae2](https://doi.org/10.3847/1538-4357/aadae2)
- Hamilton, C., & Rafikov, R. R. 2019, *MNRAS*, 488, 5512, doi: [10.1093/mnras/stz2026](https://doi.org/10.1093/mnras/stz2026)
- Heggie, D. C. 1975, *MNRAS*, 173, 729, doi: [10.1093/mnras/173.3.729](https://doi.org/10.1093/mnras/173.3.729)
- Hernquist, L. 1990, *ApJ*, 356, 359, doi: [10.1086/168845](https://doi.org/10.1086/168845)
- Hills, J. G. 1981, *AJ*, 86, 1730, doi: [10.1086/113058](https://doi.org/10.1086/113058)
- Hoang, B.-M., Naoz, S., Kocsis, B., Rasio, F. A., & Dosopoulou, F. 2018, *ApJ*, 856, 140, doi: [10.3847/1538-4357/aaafce](https://doi.org/10.3847/1538-4357/aaafce)
- Hoang, B.-M., Naoz, S., & Kremer, K. 2020, *ApJ*, 903, 8, doi: [10.3847/1538-4357/abb66a](https://doi.org/10.3847/1538-4357/abb66a)
- Jurić, M., Ivezić, Ž., Brooks, A., et al. 2008, *ApJ*, 673, 864, doi: [10.1086/523619](https://doi.org/10.1086/523619)
- Kaib, N. A., & Raymond, S. N. 2014, *ApJ*, 782, 60, doi: [10.1088/0004-637X/782/2/60](https://doi.org/10.1088/0004-637X/782/2/60)
- Kimpson, T. O., Spera, M., Mapelli, M., & Ziosi, B. M. 2016, *MNRAS*, 463, 2443, doi: [10.1093/mnras/stw2085](https://doi.org/10.1093/mnras/stw2085)
- Kopparapu, R. K., Hanna, C., Kalogera, V., et al. 2008, *ApJ*, 675, 1459, doi: [10.1086/527348](https://doi.org/10.1086/527348)
- Kozai, Y. 1962, *AJ*, 67, 591
- Kremer, K., Spera, M., Becker, D., et al. 2020, *ApJ*, 903, 45, doi: [10.3847/1538-4357/abb945](https://doi.org/10.3847/1538-4357/abb945)
- Kroupa, P. 2001, *MNRAS*, 322, 231, doi: [10.1046/j.1365-8711.2001.04022.x](https://doi.org/10.1046/j.1365-8711.2001.04022.x)
- Leibler, C. N., & Berger, E. 2010, *ApJ*, 725, 1202, doi: [10.1088/0004-637X/725/1/1202](https://doi.org/10.1088/0004-637X/725/1/1202)
- Leigh, N. W. C., Geller, A. M., McKernan, B., et al. 2018, *MNRAS*, 474, 5672, doi: [10.1093/mnras/stx3134](https://doi.org/10.1093/mnras/stx3134)
- Lidov, M. L. 1962, *Planet. Space Sci.*, 9, 719, doi: [10.1016/0032-0633\(62\)90129-0](https://doi.org/10.1016/0032-0633(62)90129-0)
- Lightman, A. P., & Shapiro, S. L. 1977, *ApJ*, 211, 244, doi: [10.1086/154925](https://doi.org/10.1086/154925)
- Liu, B., & Lai, D. 2018, *ApJ*, 863, 68, doi: [10.3847/1538-4357/aad09f](https://doi.org/10.3847/1538-4357/aad09f)
- Mandel, I. 2016, *MNRAS*, 456, 578, doi: [10.1093/mnras/stv2733](https://doi.org/10.1093/mnras/stv2733)
- Mandel, I., & de Mink, S. E. 2016, *MNRAS*, 458, 2634, doi: [10.1093/mnras/stw379](https://doi.org/10.1093/mnras/stw379)
- Mandel, I., & Smith, R. J. E. 2021, *ApJL*, 922, L14, doi: [10.3847/2041-8213/ac35dd](https://doi.org/10.3847/2041-8213/ac35dd)
- Maoz, D., Mannucci, F., & Nelemans, G. 2014, *ARA&A*, 52, 107, doi: [10.1146/annurev-astro-082812-141031](https://doi.org/10.1146/annurev-astro-082812-141031)
- Marchant, P., Langer, N., Podsiadlowski, P., Tauris, T. M., & Moriya, T. J. 2016, *A&A*, 588, A50, doi: [10.1051/0004-6361/201628133](https://doi.org/10.1051/0004-6361/201628133)
- Martinez, M. A. S., Fragione, G., Kremer, K., et al. 2020, *ApJ*, 903, 67, doi: [10.3847/1538-4357/abba25](https://doi.org/10.3847/1538-4357/abba25)
- Merritt, D. 2013, *Classical and Quantum Gravity*, 30, 244005, doi: [10.1088/0264-9381/30/24/244005](https://doi.org/10.1088/0264-9381/30/24/244005)
- Michaely, E. 2020, *MNRAS*, doi: [10.1093/mnras/staa3623](https://doi.org/10.1093/mnras/staa3623)
- Michaely, E., & Perets, H. B. 2016, *MNRAS*, 458, 4188, doi: [10.1093/mnras/stw368](https://doi.org/10.1093/mnras/stw368)
- . 2019, *ApJL*, 887, L36, doi: [10.3847/2041-8213/ab5b9b](https://doi.org/10.3847/2041-8213/ab5b9b)
- Michaely, E., & Perets, H. B. 2020, *Monthly Notices of the Royal Astronomical Society*, doi: [10.1093/mnras/staa2720](https://doi.org/10.1093/mnras/staa2720)
- Michaely, E., & Shara, M. M. 2021, *MNRAS*, 502, 4540, doi: [10.1093/mnras/stab339](https://doi.org/10.1093/mnras/stab339)
- Miller, M. C., & Hamilton, D. P. 2002, *ApJ*, 576, 894, doi: [10.1086/341788](https://doi.org/10.1086/341788)
- Moe, M., & Di Stefano, R. 2016, *ArXiv e-prints*. <https://arxiv.org/abs/1606.05347>
- Naoz, S. 2016, *ARA&A*, 54, 441, doi: [10.1146/annurev-astro-081915-023315](https://doi.org/10.1146/annurev-astro-081915-023315)
- Nomoto, K. 1982, *ApJ*, 253, 798, doi: [10.1086/159682](https://doi.org/10.1086/159682)
- . 1984, *ApJ*, 277, 791, doi: [10.1086/161749](https://doi.org/10.1086/161749)
- Olejak, A., Fishbach, M., Belczynski, K., et al. 2020, *ApJL*, 901, L39, doi: [10.3847/2041-8213/abb5b5](https://doi.org/10.3847/2041-8213/abb5b5)
- Peters, P. C. 1964, *Physical Review*, 136, 1224, doi: [10.1103/PhysRev.136.B1224](https://doi.org/10.1103/PhysRev.136.B1224)
- Petrovich, C., & Antonini, F. 2017, *ApJ*, 846, 146, doi: [10.3847/1538-4357/aa8628](https://doi.org/10.3847/1538-4357/aa8628)
- Rastello, S., Mapelli, M., Di Carlo, U. N., et al. 2021, *MNRAS*, 507, 3612, doi: [10.1093/mnras/stab2355](https://doi.org/10.1093/mnras/stab2355)
- Repetto, S., Davies, M. B., & Sigurdsson, S. 2012, *MNRAS*, 425, 2799, doi: [10.1111/j.1365-2966.2012.21549.x](https://doi.org/10.1111/j.1365-2966.2012.21549.x)
- Repetto, S., Igoshev, A. P., & Nelemans, G. 2017, *MNRAS*, 467, 298, doi: [10.1093/mnras/stx027](https://doi.org/10.1093/mnras/stx027)
- Rodriguez, C. L., Amaro-Seoane, P., Chatterjee, S., et al. 2018, *PhRvD*, 98, 123005, doi: [10.1103/PhysRevD.98.123005](https://doi.org/10.1103/PhysRevD.98.123005)
- Rodriguez, C. L., Chatterjee, S., & Rasio, F. A. 2016, *PhRvD*, 93, 084029, doi: [10.1103/PhysRevD.93.084029](https://doi.org/10.1103/PhysRevD.93.084029)
- Rodriguez, C. L., Kremer, K., Chatterjee, S., et al. 2021, *Research Notes of the American Astronomical Society*, 5, 19, doi: [10.3847/2515-5172/abdf54](https://doi.org/10.3847/2515-5172/abdf54)
- Salpeter, E. E. 1955, *ApJ*, 121, 161, doi: [10.1086/145971](https://doi.org/10.1086/145971)
- Samsing, J., MacLeod, M., & Ramirez-Ruiz, E. 2014, *ApJ*, 784, 71, doi: [10.1088/0004-637X/784/1/71](https://doi.org/10.1088/0004-637X/784/1/71)
- . 2018, *ApJ*, 853, 140, doi: [10.3847/1538-4357/aaa715](https://doi.org/10.3847/1538-4357/aaa715)
- Silber, K., & Tremaine, S. 2017, *ApJ*, 836, 39, doi: [10.3847/1538-4357/aa5729](https://doi.org/10.3847/1538-4357/aa5729)

- Stephan, A. P., Naoz, S., Ghez, A. M., et al. 2016, MNRAS, 460, 3494, doi: [10.1093/mnras/stw1220](https://doi.org/10.1093/mnras/stw1220)
- . 2019, ApJ, 878, 58, doi: [10.3847/1538-4357/ab1e4d](https://doi.org/10.3847/1538-4357/ab1e4d)
- Stone, N. C., Metzger, B. D., & Haiman, Z. 2017, MNRAS, 464, 946, doi: [10.1093/mnras/stw2260](https://doi.org/10.1093/mnras/stw2260)
- The LIGO Scientific Collaboration, the Virgo Collaboration, the KAGRA Collaboration, et al. 2021a, arXiv e-prints, arXiv:2111.03606. <https://arxiv.org/abs/2111.03606>
- . 2021b, arXiv e-prints, arXiv:2111.03634. <https://arxiv.org/abs/2111.03634>
- Vigna-Gómez, A., Toonen, S., Ramirez-Ruiz, E., et al. 2021, ApJL, 907, L19, doi: [10.3847/2041-8213/abd5b7](https://doi.org/10.3847/2041-8213/abd5b7)
- Wang, H., Stephan, A. P., Naoz, S., Hoang, B.-M., & Breivik, K. 2020, arXiv e-prints, arXiv:2010.15841. <https://arxiv.org/abs/2010.15841>
- Ye, C. S., Fong, W.-f., Kremer, K., et al. 2020, ApJL, 888, L10, doi: [10.3847/2041-8213/ab5dc5](https://doi.org/10.3847/2041-8213/ab5dc5)
- Zhu, G., Blanton, M. R., & Moustakas, J. 2010, ApJ, 722, 491, doi: [10.1088/0004-637X/722/1/491](https://doi.org/10.1088/0004-637X/722/1/491)